On the role of external force of actin filaments in the formation of tubular protrusions of closed membrane shapes with anisotropic membrane components

Luka Mesarec, Wojciech Góźdź, Samo Kralj, Miha Fošnarič, Samo Penič, Veronika Kralj-Iglič & Aleš Iglič

European Biophysics Journal
with Biophysics Letters

ISSN 0175-7571

Eur Biophys J
DOI 10.1007/s00249-017-1212-z

Springer

Eur Biophys J
DOI 10.1007/s00249-017-1212-z

ORIGINAL ARTICLE

EBSA
Biophysics in Europe

On the role of external force of actin filaments in the formation of tubular protrusions of closed membrane shapes with anisotropic membrane components

Luka Mesarec[1] · Wojciech Góźdź[2] · Samo Kralj[3,4] · Miha Fošnarič[1] · Samo Penič[1] · Veronika Kralj-Iglič[5,6] · Aleš Iglič[1,6]

Received: 14 December 2016 / Revised: 6 April 2017 / Accepted: 13 April 2017

Abstract Biological membranes are composed of different components and there is no a priori reason to assume that all components are isotropic. It was previously shown that the anisotropic properties of membrane components may explain the stability of membrane tubular protrusions even without the application of external force. Our theoretical study focuses on the role of anisotropic membrane components in the stability of membrane tubular structures generated or stabilized by actin filaments. We show that the growth of the actin cytoskeleton inside the vesicle can induce the partial lateral segregation of different membrane components. The entropy of mixing of membrane components hinders the total lateral segregation of the anisotropic and isotropic membrane components. Self-assembled aggregates formed by anisotropic membrane components facilitate the growth of long membrane tubular protrusions. Protrusive force generated by actin filaments favors strong segregation of membrane components by diminishing the opposing effect of mixing entropy.

Keywords Numerical study · Biological membranes · Vesicles · Anisotropic membrane components · Membrane tubular protrusions · Actin cytoskeleton

Special Issue: Regional Biophysics Conference 2016.

We would like to acknowledge the support from National Science Center Grant 2015/19/B/ST3/03122 and the Grants of the Slovenian Research Agency (ARRS) No. P-0232, J5-7098 and P3-0388. Prof. Nir Gov is gratefully acknowledged for help and fruitful discussions.

✉ Luka Mesarec
mesarec.luka@gmail.com

[1] Laboratory of Biophysics, Faculty of Electrical Engineering, University of Ljubljana, Tržaška 25, 1000 Ljubljana, Slovenia

[2] Institute of Physical Chemistry, Polish Academy of Sciences, Kasprzaka 44/52, 01-224 Warsaw, Poland

[3] Department of Physics, Faculty of Natural Sciences and Mathematics, University of Maribor, Koroška cesta 160, 2000 Maribor, Slovenia

[4] Jožef Stefan Institute, PO Box 3000, 1000 Ljubljana, Slovenia

[5] Laboratory of Clinical Biophysics, Faculty of Health Sciences, University of Ljubljana, Zdravstvena 5, 1000 Ljubljana, Slovenia

[6] Laboratory of Clinical Biophysics, Faculty of Medicine, University of Ljubljana, Zaloška 9, 1000 Ljubljana, Slovenia

Introduction

Biological membranes can be viewed as multicomponent systems (Israelachvili 2011; Baumgart et al. 2011). The membrane constituents themselves may generate the curvature of the membrane, which, in turn, depends on the intrinsic shape of the constituents and their interaction with other membrane constituents. The basic building block of the cell membrane is the lipid bilayer which contains many different kinds of lipids, proteins and other molecules (Singer and Nicolson 1972; McMahon and Gallop 2005; Peter et al. 2004; Saarikangas et al. 2009; Gómez-Llobregat et al. 2016; Simons and Sampaio 2011). Membrane proteins and protein-lipid complexes are examples of typical anisotropic membrane components (Iglič et al. 2007). In addition, lipid molecules, as the main component of biological membranes, should in general also be considered as anisotropic molecules (Perutková et al. 2011; Rappolt et al. 2008; Kulkarni 2012). Proteins and lipid molecules

Published online: 09 May 2017

and their complexes are able to freely move within the two-dimensional membrane (Umeda et al. 1998).

The shape of the membrane at the site of a particular membrane constituent is described by two principal membrane curvatures, while the intrinsic shape of the membrane constituent/nanodomain is characterized by the corresponding principal curvatures of the imaginary membrane that would completely fit the unconstrained constituent (Iglič et al. 2007; Kralj-Iglič et al. 2002; Fournier 1996; Kralj-Iglič et al. 1999). In general, the principal directions of these two systems may be rotated with respect to each other at the site of the constituent (Kralj-Iglič et al. 1999, 2002). If the two principal membrane curvatures at a given site are equal, the membrane shape is considered isotropic, while if they differ, it is considered anisotropic (Fournier 1996; Kralj-Iglič et al. 1996; Iglič et al. 2007; Kralj-Iglič et al. 2000). Likewise, membrane constituents with intrinsically equal/different principal curvatures are considered isotropic/anisotropic (Iglič et al. 2007; Fournier 1996; Kralj-Iglič et al. 1999, 1996, 2002; Walani et al. 2014; Mesarec et al. 2016). In general, the intrinsic shapes of membrane constituents are anisotropic (Iglič et al. 2007; Fournier 1996; Kralj-Iglič et al. 1996; Walani et al. 2014; Mesarec et al. 2016; Kralj-Iglič et al. 2006). In addition, membrane curvature at almost all points on the membrane surface is anisotropic.

Tubular protrusions of biological membranes play an important role in cellular processes. There have been many attempts to explain the growth and stability of the tubular membrane protrusions observed experimentally. For example, it has been shown that minimization of the isotropic bending energy of the membrane, considered as an isotropic two-dimensional liquid (Canham 1970; Helfrich and Naturforsch 1973), is not sufficient to explain the stability of highly curved membrane tubular protrusions (Kralj-Iglič et al. 2000, 2002; Iglič et al. 2007).

Based on the liquid mosaic model (Singer and Nicolson 1972), which described the biological membrane as a two-dimensional isotropic liquid lipid bilayer with embedded laterally mobile larger molecules, early physical models (Canham 1970; Helfrich and Naturforsch 1973) considered the membrane as a thin elastic shell; the shell was taken to have laterally isotropic properties. These models and their modifications successfully described the observed shapes of erythrocytes and phospholipid vesicles if the membrane did not exhibit highly anisotropically curved regions (reviewed in Seifert 1997). To include also shapes with such regions, a model considering also deviatoric elasticity was proposed on the continuum level (Fischer 1992, 1993), introducing the spontaneous membrane warp as a parameter. However, the author Fischer (1992) and Fischer (1993) considered that its value was zero arguing that biological membranes as observed in experiments were locally flat. That is, the existence of membranous nanostructures was then not yet widely acknowledged. In 1996, a deviatoric elasticity model (DE) was proposed, which takes into account the anisotropic properties of membrane components (Kralj-Iglič et al. 1996; Fournier 1996. Deviatoric elasticity was derived from a single-constituent energy by applying methods of statistical physics (Kralj-Iglič et al. 1996, 1999; Fournier and Galatola 1998; Kralj-Iglič et al. 2000, 2006; Fournier 1996). The deviatoric contribution to the membrane free energy resulted from in-plane orientational ordering of the anisotropic constituents. Membrane constituents/domains in the DE model can be isotropic or anisotropic, which is a general approach (Hägerstrand et al. 2006; Baumgart et al. 2011; Helfrich 1988; Fournier 1996; Kralj-Iglič et al. 1999, 2002; Fournier and Galatola 1998; Walani et al. 2014; Kralj-Iglič et al. 2002), not limited by the assumption of isotropic elasticity. By applying this model it was shown that the deviatoric effect stabilizes shapes of cells/vesicles with strongly anisotropically curved regions, such as shapes with thin tubular protrusions (Kralj-Iglič et al. 2002; Fournier and Galatola 1998; Fournier 1996; Iglič et al. 2006; Perutková et al. 2010; Kabaso et al. 2012, 2012; Bobrovska et al. 2013; Iglič et al. 2005, 2015) and narrow necks (Kralj-Iglič et al. 1999, 2006; Kralj-Iglic 2012; Iglič et al. 2007, 2007).

Tubular membrane protrusions could also be a consequence of external force acting on the membrane. External force to the membrane surface can be generated experimentally by the cantilever of an atomic force microscope (Boulbitch 1998). In other experiments, vesicles are aspirated into a micropipette and a tether is pulled out of the surface by gravitational forces on small glass beads that have adhered to the vesicle surface (Bo and Waugh 1989). The force on the tether can be generated also by an electromagnet acting on a paramagnetic bead attached to the vesicle surface (Heinrich and Waugh 1996). In such experiments, the membrane of a phospholipid vesicle is point-attached on one side to the tip of a glass micropipette and on the other side to a paramagnetic bead (Heinrich et al. 1999). By application of hydrodynamic flow, lipidic tethers can be generated from the membranes of giant unilamellar vesicles (Borghi et al. 2003). By measuring the tether (tube) force, it is also possible to determine the bending rigidity and the lateral membrane tension of vesicles (Cuvelier et al. 2005).

Cell membrane can also be deformed in small regions when subjected to a localized force or torque caused by an integral protein (Fošnarič and Iglič 2006), a receptor or a cell-kicking instrument (Boulbitch 1998). In some experiments with liposomes, actin polymerization, which leads to the growth of elongated actin filaments beneath the membrane, is the origin of the protrusive force (Miyata et al. 1999; Häckl et al. 1998). The elongating actin filaments "push out" the cell/vesicle membrane in the

direction normal to the membrane surface (Miyata et al. 1999; Boulbitch 1998), which may result in membrane tubulation (Gov and Gopinathan 2006; Veksler and Gov 2007). However, it is still not fully understood whether membrane protrusions reply on the force of polymerizing actin filaments inside the cell, or if they membrane protrusions are just stabilized by actin filaments (Yang et al. 2009).

Liposome shapes with tubular protrusions, i.e., the so-called ϕ shapes, were observed also in experiments with tubulin inside the liposomes, as the consequence of tubulin self-assembly into rod-like structures (microtubules) (Downing and Nogales 1998; Wade and Hyman 1997) inside the vesicles (Emsellem et al. 1998; Elbaum et al. 1996; Fygenson et al. 1997). The polymerization of microtubules confined within the vesicles can lead to quasistatic deformation of lipid vesicles (Fygenson et al. 1997). As the microtubule inside the vesicle grows longer, a pair of long, narrow membrane sleeves appears, sheathing the microtubule ends, which results in the formation of ϕ shape (Fygenson et al. 1997), observed also in cellular systems (Iglič et al. 2006, 2001). The growth of encapsulated microtubules inside the vesicles can deform vesicles also into other morphologies such as ovals, cherries, dumbbells, lemons and pearls (Emsellem et al. 1998).

Some experimental and theoretical studies suggest that the membrane tubular protrusions can be stable without actin filaments (Kralj-Iglič et al. 2000, 2002; Iglič et al. 2007; Kabaso et al. 2012). It has been suggested that actin filaments are not necessary for the generation of the membrane protrusions, but only for the stabilization of the protrusion, which could be induced by self-assembly of anisotropic membrane components, for example BAR protein domains (Noguchi 2016; Yang et al. 2009; Frost et al. 2009; Simunovic et al. 2015; Scita et al. 2008). The BAR domain superfamily consists of BAR/N-BAR, F-BAR and I-BAR domains, each enforcing a different local curvature on the membrane surface (Suetsugu 2010). The interaction between proteins and membranes can result in shape deformations and topology changes of cell/vesicle membranes, which are important for many biological processes, such as cell signaling, cell division, and protein trafficking (Ayton and Voth 2010; Davtyan et al. 2016). This effect is known as protein-mediated membrane remodeling (Ayton and Voth 2010; Davtyan et al. 2016). BAR domain-induced membrane remodeling can result in liposome tubulation and vesiculation (Ayton et al. 2009; Ahmed et al. 2010; Zimmerberg and McLaughlin 2004).

It has been found that the actin cytoskeleton may be necessary for a long-term stabilization of membrane tubular protrusions (Yang et al. 2009). The cytoskeleton is in general a network of protein filaments spanning the cytoplasm (Umeda et al. 1998). It has been shown that a lipid bilayer can drive the emergence of bundled actin filament protrusions from branched actin filament networks, which indicates an active participation of the membrane in organizing the actin filaments (Liu et al. 2008).

The coupling of actin and curved proteins can also induce instabilities, such as pearling (Jelerčič 2015; Shlomovitz 2008). It has been shown that curved proteins that recruit actin polymerization can destabilize the membrane tube; either due to fast squeeze (leading to pearling) of a uniform actin for coat (Jelerčič 2015), or due to the inward force forming denser protein rings that shrink the tube (Shlomovitz 2008). The pearling instability is important because it can initiate fission of the membrane tube into vesicles. The actin polymerization may also provide the additional constrictive force needed for the robust instability of the membrane tubes (Jelerčič 2015).

In this paper, we were mainly interested in the influence of actin filaments on the calculated vesicle shapes. Actin filaments are far less rigid structures than microtubules (Isambert et al. 1995; Venier et al. 1994), which may imply that actin filaments play more of a supporting role, rather than being active elements generating the growth of membrane tubular protrusions (Miyata et al. 1999). We applied the deviatoric elasticity (DE) model to study the role of anisotropic membrane domains in the formation and stability of the membrane tubular protrusions. We also studied the effect of the external force on the calculated vesicle shapes, which could be, among others, a consequence of elongating actin filaments inside of the vesicle. Within the DE model, we explained the stability of experimentally observed membrane tubular protrusions even without the application of external force, if the role of anisotropic membrane components was taken into account. We pointed out the role of local actin force in the process of lateral segregation of membrane constituents with different intrinsic curvatures (shapes).

The structure of the paper is as follows. In Sect. 2, we describe the theoretical models of vesicle shape used in this work. In Sects. 2.1 and 2.2, we briefly describe the numerical procedures used to calculate closed vesicle shapes with minimal membrane free energy. In Sect. 3, we present and discuss the results of our study. We compare the vesicle shapes, calculated within the DE model, with and without taking into account the entropy of mixing. The influence of the application of the local force of actin filaments on the shape and stability of vesicle protrusion was also considered. For comparison, we also show the shape of a non-axisymmetric vesicle, calculated by Monte Carlo simulations within the model of isotropic membrane elasticity. Finally, we summarize the main conclusions of our study in Sect. 4.

Model and methods

We consider a membrane composed of two different components A and B, which are characterized by the intrinsic principal curvatures C^i_{1m} and C^i_{2m}, where $i = A, B$. The bending energy of a membrane in the DE model may be written as Iglič et al. (2005), Fošnarič (2008) and Bobrovska et al. (2013):

$$F_b = \int_S \kappa(\phi)\left[(H - H_m(\phi))^2 + (D - D_m(\phi))^2\right] \mathrm{d}S, \quad (1)$$

where $\mathrm{d}S$ is an infinitesimal element of the vesicle area S and ϕ is the local relative area density of the component A. The local relative area density of the component B is therefore $(1 - \phi)$. $H = (C_1 + C_2)/2$ is the membrane mean curvature and $D = |C_1 - C_2|/2$ is the membrane curvature deviator (Kralj-Iglič et al. 2000; Fischer 1992, 1993; Kralj-Iglič et al. 1996, 1999; Fournier 1996; Walani et al. 2014), where C_1 and C_2 stand for the membrane principal curvatures. We assume that the bending rigidity $\kappa(\phi)$, the intrinsic mean curvature $H_m(\phi)$ and the curvature deviator $D_m(\phi)$ depend linearly on the local relative area density of the component A (ϕ):

$$\kappa(\phi) = (\kappa^A - \kappa^B)\phi + \kappa^B, \quad (2)$$

$$H_m(\phi) = (H^A_m - H^B_m)\phi + H^B_m, \quad (3)$$

$$D_m(\phi) = (D^A_m - D^B_m)\phi + D^B_m, \quad (4)$$

where κ^i is the bending rigidity of the component i, $H^i_m = (C^i_{1m} + C^i_{2m})/2$ is the intrinsic mean curvature of the component i and $D^i_m = |C^i_{1m} - C^i_{2m}|/2$ is the intrinsic curvature deviator of the component i, where $i = A, B$. Membrane constituent i is considered isotropic when its intrinsic deviatoric curvature $D^i_m = 0$ ($C^i_{1m} = C^i_{2m}$). Note that Eq. (1) assumes that the principal system of the actual local membrane curvature tensor and the intrinsic membrane curvature tensor coincide everywhere on the surface of the vesicle (Iglič et al. 2005), i.e., the anisotropic membrane components are perfectly oriented.

The second part of the membrane free energy is associated with the entropy of mixing (Hägerstrand et al. 2006; Fošnarič 2008; Bobrovska et al. 2013):

$$F_{mix} = \frac{k_B T}{a_0} \int_S [\phi \ln \phi + (1 - \phi) \ln (1 - \phi)] \mathrm{d}S, \quad (5)$$

where k_B is the Boltzmann constant, T is the absolute temperature and a_0 is the area of a single nanodomain. The free energy functional is the sum of energy contributions defined by Eqs. (1) and (5):

$$F = F_b + F_{mix}. \quad (6)$$

Numerical minimization

In this work, we first considered axisymmetric vesicle shapes with the rotational symmetry about the z-axis. To describe the surface of the axisymmetric vesicle, we need to define a vesicle profile curve in the $r - z$ plane (Fig. 1). The vesicle surface is constructed by the rotation of the profile curve around the z-axis by the angle $\varphi = 2\pi$. The vesicle profile curve is parameterized with the angle between the line tangent to the profile curve and the plane that is perpendicular to the axis of rotation z, $\theta(s)$, where s stands for the arc length of the profile curve (Góźdź 2004) (Fig. 1). If the function $\theta(s)$ is known, the radius $r(s)$ and the height $z(s)$ of the shape profile are calculated according to:

$$r(s) = \int_0^s \cos(\theta(s'))\, \mathrm{d}s', \quad (7)$$

$$z(s) = \int_0^s \sin(\theta(s'))\, \mathrm{d}s'. \quad (8)$$

The function describing the shape contour $\theta(s)$ (see Fig. 1) is approximated by Fourier series (Góźdź 2005),

$$\theta(s) = \theta_0 \frac{s}{L_s} + \sum_{i=1}^{N} a_i \sin\left(\frac{\pi}{L_s} i \cdot s\right), \quad (9)$$

where L_s is the length of the shape profile (Fig. 1), N is the number of Fourier modes and a_i are the Fourier amplitudes. For the axisymmetric closed vesicle shape,

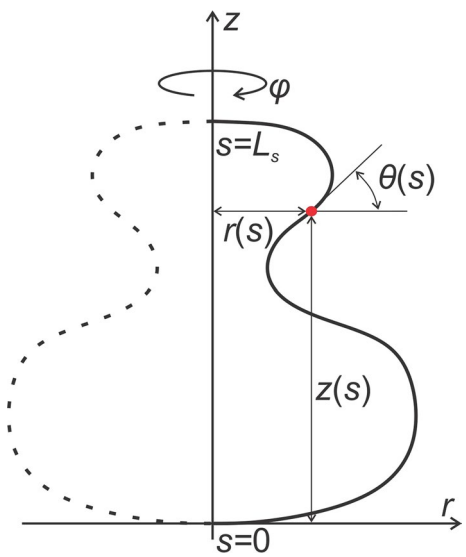

Fig. 1 The vesicle profile in $r - z$ plane, where $r(s)$ is the radius and $z(s)$ the height of the shape profile at the given arc length s. $r(s)$ and $z(s)$ are calculated with the aid of $\theta(s)$ from Eqs. (7) and (8). L_s is the length of the shape profile and φ is the angle of rotation around the z-axis

we apply the following boundary conditions: $\theta(0) = 0$, $\theta(L_s) = \pi$, $r(0) = r(L_s) = 0$, which guarantee that the profile is smooth and the vesicle is closed. θ_0 is the angle at the north pole of the vesicle (Fig. 1), $\theta_0 = \theta(L_s) = \pi$. In analogy to the area density profile for laterally separated mixtures, we postulate that the local relative area density of the component A has the form:

$$\phi(s) = \left(\phi_2^A - \phi_1^A\right)[-\tanh(\xi(s - s_0)) + 1]/2 + \phi_1^A, \quad (10)$$

where the vesicle surface is divided into two regions, which are characterized by the maximal and the minimal possible local area densities of the component A, ϕ_2^A and ϕ_1^A, respectively. The parameters ξ and s_0 determine the width and the position of the boundary between those regions (Góźdź 2006; Góźdź et al. 2012; Bobrovska et al. 2013). The constraint on the average relative area density of the component A ϕ_{ave} is calculated as the following integral over the surface of the vesicle:

$$\phi_{ave} = \int_0^{2\pi} \mathrm{d}\varphi \int_0^{L_s} \phi(s) r(s) \mathrm{d}s \, / S, \quad (11)$$

where S is the surface area of the vesicle. The remaining surface area of the vesicle (not covered by the component A) is completely covered by the component B.

The study also explores the impact of external force on the vesicle shapes. Such a force may be generated experimentally by a cantilever of an atomic force microscope (Boulbitch 1998), or it may be a consequence of growing actin cytoskeleton inside of cells/vesicles (Miyata et al. 1999). In our study, actin cytoskeleton is modeled as a thin rod-like structure, which stretches the vesicle (see Fig. 2). In the model, the vesicle vertical height h is always longer than or equal to the cytoskeleton length d (see Fig. 2). In the minimization procedure, we add a constraint of minimal vertical distance between the poles of the vesicle $z(L_s) \geq d$, where d is the minimal vertical distance equal to the length of actin rod-like structure inside the vesicle (Góźdź 2004; Góźdź et al. 2012) (Fig. 2).

With the aid of Eqs. (9) and (10), the minimization of the free energy functional (Eq. 6) is replaced by the minimization of a function with many variables. In our case, these variables are the Fourier amplitudes a_i, the shape profile length L_s, and the parameters ξ, s_0, ϕ_2^A, ϕ_1^A. The principal curvatures C_1 and C_2, for axisymmetric shapes, are given as $\frac{d\theta(s)}{ds}$ and $\frac{\sin(\theta(s))}{r(s)}$, respectively. During the minimization procedure, the vesicle surface area S and the volume V are kept constant in order to set a fixed value of the vesicle reduced volume v. The reduced volume v is defined as the ratio of the vesicle volume to the volume of the sphere with the same surface area as a given vesicle.

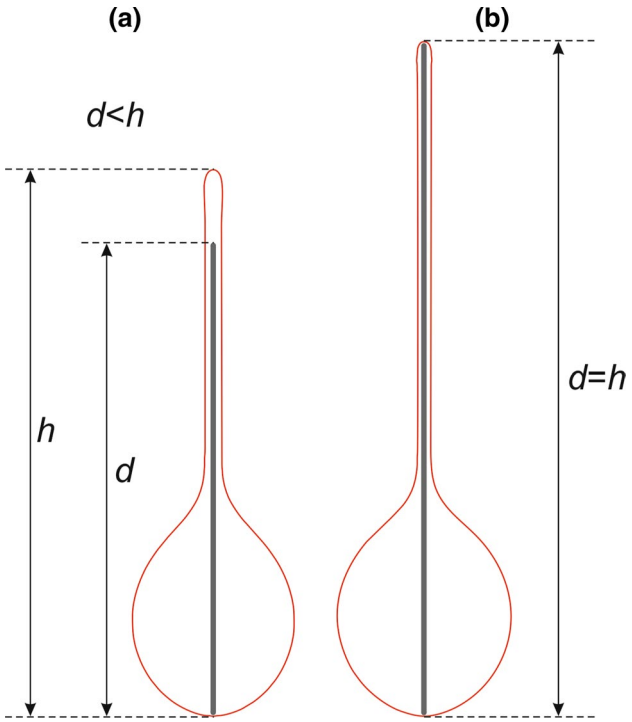

Fig. 2 Schematic presentation of the actin rod-like structure inside the axisymmetric vesicle. The length of the actin rod is denoted by d, and the vertical height of the vesicle by h. **a** Represents the case without an external local force of actin, where the actin rod-like structure inside the vesicle is shorter than the vesicle height. **b** Represents the axisymmetric vesicle, which is stretched due to the local force of the elongated actin rod

The equilibrium vesicle shapes are obtained by numerical minimization of the membrane energy F (Eq. 6) for fixed values of the reduced volume v, the average relative area density of the component A ϕ_{ave}, and the minimal vertical distance between the poles of the vesicle d. Note that the direct interactions between membrane components are not considered within the numerical minimization procedure. The direct interactions between nearest neighboring membrane components could be taken into account in the most simple way within the Bragg-Williams approximation (Hill 1986; Hägerstrand et al. 2006; Veksler and Gov 2007; Kabaso et al. 2012; Iglič et al. 2015) by considering an additional energy term proportional to ϕ^2.

As a result of the described minimization procedure, we obtain the functions $\theta(s)$ and $\phi(s)$, which describe the shape of the vesicle and the relative area density distribution of the membrane components A and consequently also the components B. We visualize the relative local area densities of the components A and B with a color code. All lengths in the model are scaled with respect to R, which is the radius of the sphere with the same surface area as the surface of the investigated vesicle.

Monte Carlo method

For comparison, we also performed Monte-Carlo (MC) simulations to simulate the non-axisymmetric vesicle shapes in thermodynamical equilibrium.

To this end, the membrane of the vesicle is simulated by the set of 3127 vertices linked with bonds of flexible length to form a closed, randomly triangulated, self-avoiding network (Gompper and Kroll 1996, 2004; Ramakrishnan et al. 2011; Penič et al. 2015). The bond lengths are allowed to vary between their minimal value $d_{\min}$ and maximal value $1.7\,d_{\min}$. All vertices experience a hard-core repulsive potential at their mutual distances $d_{\min}$.

All membrane components are isotropic, $D_m^A = D_m^B = 0$. Among them 80% of membrane components have zero intrinsic curvature ($H_m^A = 0$) and the remaining 20% have intrinsic mean curvature $H_m^B = 1/d_{\min}$. The bending rigidity $\kappa^A = \kappa^B = 30\,k_BT$. With the MC simulation approach we also consider direct interactions between components B. If the two vertices representing components B are nearest neighbors, an addition energy term $-\alpha k_BT$ accounts for their bond. For reasons of simplicity we selected $\alpha = 1$.

Note that besides the confined bond lengths and the hard-core repulsive potential between vertices of the network, there are no additional constraints on the shape of the vesicle. A randomly triangulated network allows bond-flips (Gompper and Kroll 2004), accounting for the in-plane mobility of the components (fluid membrane). The system is initially thermalized and then observed in thermal equilibrium.

Results and discussion

We studied the influence of the reduced volume, actin filament local force and the anisotropy of the membrane components on the calculated shapes of the vesicles. The vesicle shapes were calculated numerically as described in Sect. 2.1. The influence of the entropy of mixing of membrane components [Eq. (5)] on the calculated vesicle shapes was thoroughly investigated. The degree of lateral component separation of thje membrane components in vesicles with tubular protrusions was studied for different values of the model parameters. Finally, vesicle shapes with highly curved isotropic membrane inclusions were calculated for comparison, also for non-axisymmetric vesicle shapes, using MC simulations.

In the present theoretical study, the membrane contains isotropic and anisotropic components. Examples of possible isotropic and anisotropic membrane components are schematically shown in Fig. 3. Locally the membrane bending energy F_b [Eq. (1)] is minimal if the membrane components perfectly fit into the membrane. For example,

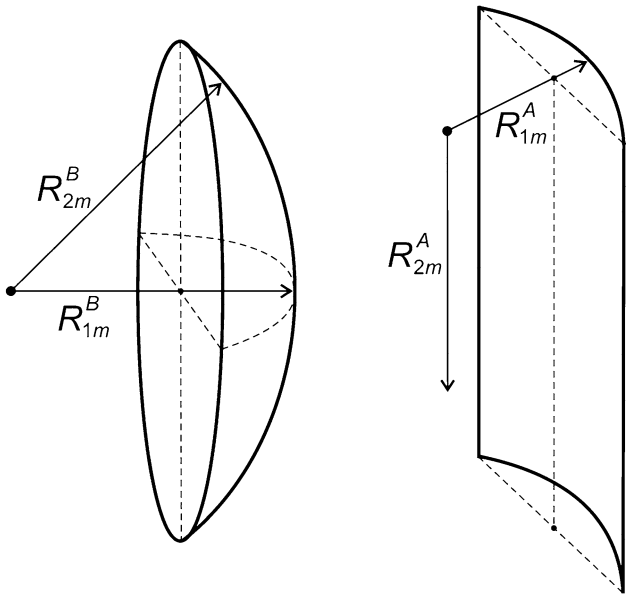

Fig. 3 Schematic presentation of isotropic spherical (*left*) and anisotropic cylindrical (*right*) membrane component. Principal radii R^i_{1m} and R^i_{2m} are linked to the principal curvatures: $C^i_{1m} = 1/R^i_{1m}$, $C^i_{2m} = 1/R^i_{2m}$, where $i = A, B$. For isotropic spherical component, both principal curvatures are equal and different than zero: $C^B_{1m} = C^B_{2m} \neq 0$, while for anisotropic cylindrical: $C^A_{1m} \neq 0$, $C^A_{2m} = 0$

the isotropic components with intrinsic principal curvatures C^B_{1m} and C^B_{2m} (left side in Fig. 3) have the lowest energy, when they are part of the spherical membrane surface with principal curvatures $C_1 = C^B_{1m}$ and $C_2 = C^B_{2m}$. On the other hand, anisotropic cylindrical components (right side in Fig. 3) have a preference for membrane regions of cylindrical shape and therefore, tend to induce membrane tubular protrusions (Fig. 4).

Figure 4 shows the axisymmetric vesicle shapes calculated for different values of the reduced volume v. The average relative area density of anisotropic components A was set to $\phi_{ave} = 0.15$. The remaining surface area of the vesicle is covered by isotropic components B. The entropy of mixing of different membrane constituents was not taken into account in Fig. 4. For $v = 1$, the vesicle, according to the definition of the reduced volume, can only have a spherical shape. Spherical membranes have the same principal curvatures C_1 and C_2 everywhere on their surface, therefore, the isotropic and anisotropic components are homogeneously mixed over the whole surface. As the value of the reduced volume gets smaller, different membrane components start to assemble into separate regions. The anisotropic components try to form tubular protrusions (see Fig. 4). The lateral segregation of two membrane components A and B is most prominent at $v = 0.90$ (Fig. 4). The predicted lateral segregation of membrane components is not complete, however. Almost all anisotropic components

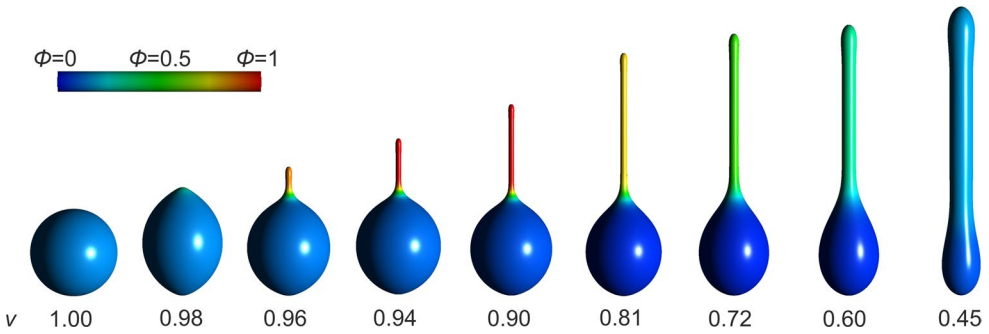

Fig. 4 Vesicle shapes without inner cytoskeleton element calculated for different values of the reduced volume v. Shapes were calculated within the deviatoric elasticity model of the membrane for the following values of model parameters: $\phi_{ave} = 0.15$, $H_m^B = 1$, $D_m^B = 0$, $H_m^A = 8$, $D_m^A = 8$, $\kappa^A = 8\,\kappa^B$ and $\kappa^B = 30\,k_BT$. The entropy of mixing of different membrane components was not taken into account

are accumulated in the tubular protrusion (red color), while most of the isotropic components reside outside this region, i.e., in the spherical part of the vesicle (dark blue color). For values of the reduced volume smaller than 0.90 ($v < 0.90$), the components A and B undergo greater mixing. As the radius of the tubular protrusion is increasing with decreasing v, the local relative area density of isotropic components in the protruding membrane region increases, because the curvature of the protrusion becomes less anisotropic, i.e., less energetically favorable for anisotropic component A and more favorable for isotropic component B. At $v = 0.45$, the isotropic and anisotropic components are almost homogeneously distributed over the whole membrane area again.

Next, we investigated the effect of an external pulling or pushing force on the calculated axisymmetric shapes of vesicles at the fixed value of the reduced volume $v = 0.78$ (Fig. 5). Such force could be applied experimentally (Boulbitch 1998) or it may be a consequence of a growing actin cytoskeleton inside of the cell (Miyata et al. 1999). The average relative area density of anisotropic components A was again set to $\phi_{ave} = 0.15$ and the entropy of mixing was again not taken into account. The actin cytoskeleton is modeled as a single actin rod-like structure (Fig. 5), which is stretching the membrane of the vesicle (see also Fig. 2). Figure 5 shows the vesicle shapes calculated for different lengths of the actin rod-like structure inside the vesicle. The calculated shape of the vesicle on the left side in Fig. 5 is not influenced by the actin force because the length of the actin rod-like structure inside the vesicle is shorter than the height of the vesicle. The other three calculated shapes in Fig. 5 are influenced by the actin rod-like structure, which is in these cases long enough to stretch the vesicles. As the actin rod-like structure grows, the tubular protrusion gets thinner and longer (Fig. 5). The formation of a thinner and longer tubular protrusion are the only way for the vesicle to stretch and at the same time to keep the value of the reduced volume constant. Thinner tubular protrusion is energetically favorable for highly anisotropic membrane components, but not favorable for isotropic components.

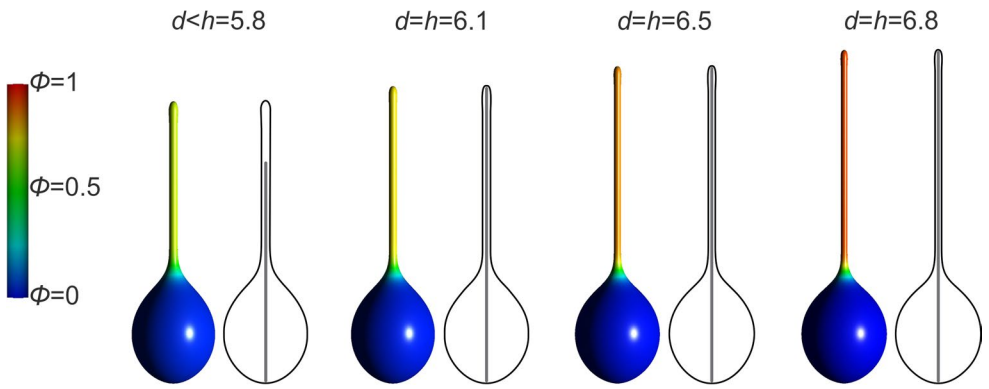

Fig. 5 Vesicle shapes calculated for different lengths of the actin rod-like structure (indicated with the *grey lines* inside the vesicles) inside the vesicle, where d is the length of the actin rod and h is the height of the vesicle. Shapes were calculated within the deviatoric elasticity model for the following values of parameters: $v = 0.78$, $\phi_{ave} = 0.15$, $H_m^B = 1$, $D_m^B = 0$, $H_m^A = 8$, $D_m^A = 8$, $\kappa^A = 8\,\kappa^B$ and $\kappa^B = 30\,k_BT$. The entropy of mixing of different membrane components was not taken into account

This is why we predicted that the local relative area density of anisotropic components in the tubular protrusion increases as the protrusion gets thinner. The vesicle shape on the right hand side of Fig. 5 ($d = h = 6.8$) has nearly the largest possible height at a given value of v. The vesicle can not be stretched much further at a given value of v, without significant increase of membrane energy (which would destabilize the shape) as it is already very close to the limit shape composed of a spherical main body and cylindrical protrusion (Mesarec et al. 2016; Perutková et al. 2010; Iglič and Kralj-Iglič 1999).

In the following figure (Fig. 6), we present the effect of the entropy of mixing of membrane components on the calculated closed membrane shapes. Again, the vesicle shapes were calculated for different values of v, with the average relative area density of anisotropic components A set to $\phi_{ave} = 0.15$. The relative importance of the entropy contribution is determined by the area of a single nanodomain a_0 and the parameter R, which is defined as the radius of the sphere with the same surface area as the surface of the investigated vesicle [see Eq. (5)]. In Figs. 4 and 6, tubular protrusions occur at similar values of v. For the calculated shapes with high ($v > 0.96$) and relatively low ($v < 0.60$) values of the reduced volume, the isotropic and anisotropic components are almost homogeneously distributed over the whole surface (Fig. 6). It should be noted that these shapes (for $v > 0.96$ and $v < 0.60$) are not strongly influenced by the entropy of mixing (see Figs. 4, 6). For the other values of the reduced volume ($0.60 \leq v < 0.96$), we observe a lateral segregation of membrane components and the formation of tubular protrusions. The predicted curvature driven lateral segregation of the isotropic and anisotropic components is less prominent if the mixing entropy is taken into account (see Figs. 4, 6). The entropy contribution to the free energy functional F_{mix} [Eq. (5)] enforces different kinds of membrane components to intermix more strongly with each other, for which reason we do not predict shapes with a high degree of the membrane component lateral separation in Fig. 6. Vesicles, calculated with the entropy of mixing taken into account, also have wider tubular protrusions, because of the relatively high local relative area density of isotropic components in the region of a tubular protrusion.

In Fig. 7, we studied the influence of application of actin force on the calculated vesicle shapes with and without the entropy of mixing. Shapes were determined for reduced volume $v = 0.90$ and the average relative area density of anisotropic components $\phi_{ave} = 0.15$. The

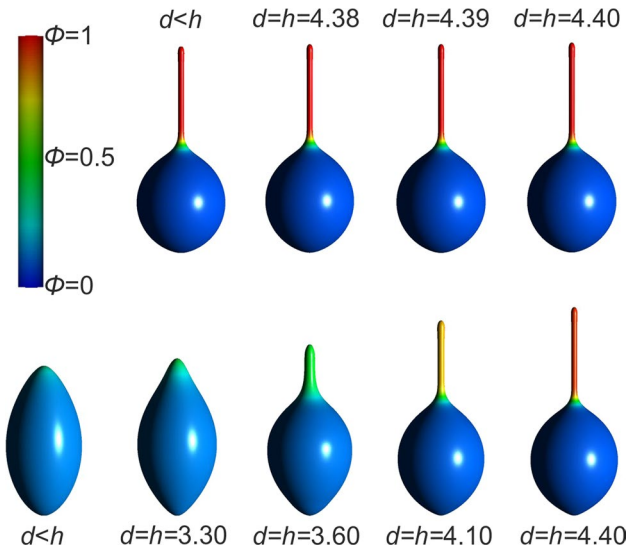

Fig. 7 Vesicle shapes calculated for different lengths of the actin rod-like structure inside the vesicle, where d is the cytoskeleton length and h is the height of the vesicle. The entropy of mixing of different membrane components was taken into account for the vesicles in the second row only, but not also for the vesicles in the first row. Shapes were calculated within the deviatoric elasticity model for the following values of model parameters: $v = 0.90$, $\phi_{ave} = 0.15$, $H_m^B = 1$, $D_m^B = 0$, $H_m^A = 8$, $D_m^A = 8$, $\kappa^A = 8\,\kappa^B$, $\kappa^B = 30\,k_BT$, $R = 250$ nm and $a_0 = 100$ nm^2

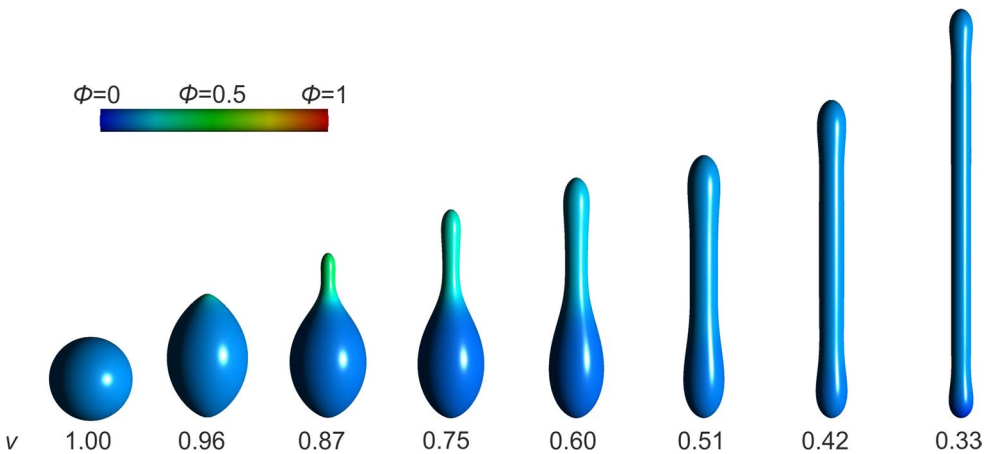

Fig. 6 Vesicle shapes calculated for different values of the reduced volume v, where the entropy of mixing is taken into account in minimization of the membrane free energy. Shapes were calculated within the deviatoric elasticity model for the following values of model parameters: $\phi_{ave} = 0.15$, $H_m^B = 1$, $D_m^B = 0$, $H_m^A = 8$, $D_m^A = 8$, $\kappa^A = 8\,\kappa^B$, $\kappa^B = 30\,k_BT$, $R = 250$ nm and $a_0 = 100$ nm^2

vesicles in the first row in Fig. 7 were calculated without considering the entropy of mixing, while for the shapes in the second row, the entropy of mixing of different membrane components was taken into account in minimization of the membrane free energy. The vesicle shapes on the left side in both rows in Fig. 7 represent the vesicles with an inner actin rod-like structure which is shorter than the height of the vesicle ($d < h$). These two vesicles are therefore not stretched by actin force. The noticeable difference between the calculated shapes of the vesicles for $d < h$ in both rows in Fig. 7 is due to the effect of mixing entropy. Without the influence of mixing entropy, the predicted lateral segregation of the membrane components A and B is very prominent, even without the application of actin force (see the shapes in the upper row in Fig. 7). The anisotropic components are nearly completely located in the protrusion (red color), while the isotropic components reside in the spherical part of the vesicle (dark blue color). The membrane of the vesicles in the first row in Fig. 7 is not stretched substantially when actin force is applied because the predicted vesicle shapes would be quite similar, i.e., close to the limit shape with a spherical bottom and a cylindrical protrusion.

Figure 7 shows that for $v = 0.90$, the membrane constituents of both kinds can not laterally segregate strongly enough to form a tubular membrane protrusion without the application of actin force if the influence of entropy of mixing is taken into account (see the first shape in the second row in Fig. 7, where $d < h$). The entropy of mixing enforces the anisotropic and isotropic membrane constituents to intermix. In the second row in Fig. 7 we therefore analyze the effect of the actin pushing force on the vesicle shapes if the entropy of mixing is taken into account. As the inner rod-like actin structure grows longer, the isotropic and anisotropic membrane components laterally segregate more strongly and the formation of a tubular protrusion is facilitated. To conclude, even when for higher values of vesicle relative volumes the mixing entropy is taken into account, the equilibrium vesicle shapes with a high degree of the membrane component lateral segregation are possible if actin force is applied. For longer actin rods, the calculated vesicle shapes with the mixing entropy of membrane components taken into account become very similar to those shapes calculated without considering the entropy of mixing (Fig. 7). For longer actin rod-like structures, the vesicle tubular protrusion gets thinner and elongated, because this is the only energetically favorable way for the vesicle to stretch and to keep the value of the reduced volume v constant at the same time.

Thin tubular membrane protrusions, generated by elongated actin rods, are energetically favorable also due to accumulation of anisotropic membrane components in the protrusion. Namely, when the tubular protrusion gets thin enough, the anisotropic components strongly accumulate in the protrusion, which leads to nearly complete lateral separation of the isotropic and anisotropic membrane constituents. The described effect can in some cases prevail over the entropy effect. A similar but not identical phenomenon was observed in Veksler and Gov (2007). When there is no interaction between membrane components and when the relative cell volume is high, the intrinsic curvature of isotropic components alone is not strong enough to offset the entropy of mixing Veksler and Gov (2007). Only with the addition of an actin cytoskeleton force, it is possible to explain strong segregation of isotropic membrane components when the entropy of mixing is taken into account (Veksler and Gov 2007). On the contrary, in the case of anisotropic membrane components, the intrinsic curvature alone can be strong enough to offset the entropy of mixing, but only for some values of the vesicle reduced volume, corresponding to wider tubular protrusions as shown in Fig. 6. To predict thinner tubular protrusions, application of actin force is needed (Fig. 7) or the anisotropy should be stronger (Kralj-Iglič et al. 2002, 2005).

Note that the complexity of the problems addressed in this article can be further increased if the higher degree of freedom of the membrane in-plane order is taken into account (MacKintosh and Lubensky 1991; Kralj-Iglič et al. 2000, 2006; Jesenek et al. 2013), which is often realized in biological membranes. Orientational ordering of anisotropic membrane constituents can be considered also within the deviatoric elasticity model, which is used in this paper. Nevertheless, Eq. (1) represents a simplified case, where it is assumed that anisotropic membrane components are always oriented in the energetically most favorable way.

In-plane ordering and deformation in the membranes due to the tilt of lipid tails was first considered by Helfrich, Lubensky and Prost (Helfrich 1988; Lubensky and Prost 1992). In biological membranes, the tails of lipid molecules may tilt relative to the surface normal and develop hexatic orientational ordering (Smith et al. 1988). Tilted bilayers tend to have both tilt and hexatic order (Smith et al. 1988). Lipid tilt deformation and lipid tilt degree of freedom play an important role in the local lipid deformation around the membrane embedded anisotropic and isotropic proteins which can locally soften a lipid bilayer membrane (Fošnarič and Iglič 2006) and can also determine the character of the depletion forces between membrane embedded proteins (Bohinc et al. 2003). The isotropic and anisotropic bending moduli of the membrane with isotropic and anisotropic membrane embedded inclusions may strongly depend on lipid tilt, splay and compression elastic moduli (Bohinc et al. 2003). The lipid tilt deformation is also closely related to the observed hexatic order/phases in lipid bilayers, with long range bond orientation order and

short-range positional order (Bernchou et al. 2009). Hexatic tilt order may persist in lipid bilayers and can possibly rationalize the textures observed in gel domains (Bernchou et al. 2009). The in-plane orientational ordering in hexatic membranes has been also experimentally observed (Bernchou et al. 2009), proving the concept of anisotropic membrane elasticity and orientational ordering of membrane components, utilized in the present work.

Some classes of membrane inclusions, for example, antimicrobial peptides and BAR protein domains, could also exhibit in-plane ordering (Zimmerberg and Kozlov 2006). The anisotropic banana-shaped BAR protein domains may, due to their in-plane (nematic) ordering (Gómez-Llobregat et al. 2016), stabilize thin membrane protrusions (Frost et al. 2009; Simunovic et al. 2015; Mesarec et al. 2016). A possible origin of anisotropy of other membrane mechanical properties besides the anisotropic bending properties, like the anisotropy of the membrane area stretching modulus, may be membrane attached protein scaffolds with oriented fibers or clusters of oriented membrane attached anisotropic proteins, such as BAR domain proteins (Mesarec et al. 2016; Walani et al. 2014).

Coupling between the in-plane orientational ordering and the membrane local curvature may lead to the formation of experimentally observed nanotubular membrane protrusions (Kralj-Iglič et al. 2000, 2002) which cannot be theoretically explained within the Helfrich-Canham isotropic membrane bending model (Helfrich and Naturforsch 1973; Canham 1970; Seifert 1997), but only within the model of anisotropic membrane elasticity (Fischer 1992; Kralj-Iglič et al. 1996; Fournier 1996; Kralj-Iglič et al. 1999; Fournier and Galatola 1998; Walani et al. 2014), utilized also in the present work. Accordingly, Fig. 8 shows the non-axisymmetric vesicle shape without inner actin cytoskeleton, calculated by MC simulations for the membrane composed of two isotropic constituents, where one component has high intrinsic curvature (red color). It can be observed that the MC predicted vesicle shape has only undulating (necklace-like) membrane protrusions and no tubular protrusions.

Moreover, it was experimentally proved (Kralj-Iglič et al. 2000, 2005) that in red blood cells, the tubular budding of the membrane can be induced only by anisotropic dimeric amphiphiles intercalated in the red blood cell membrane, but not by isotropic monomeric amphiphiles which can induce only spherical budding of the membrane. These experimental results strongly support the theoretical results presented in this work, showing that without the actin force only anisotropic membrane components may facilitate the formation of tubular membrane protrusions. The comparison of theoretical and experimental results (Perutková et al. 2009, 2011; Rappolt et al. 2008) indicates that the concept of the anisotropic shape of lipid molecules and their

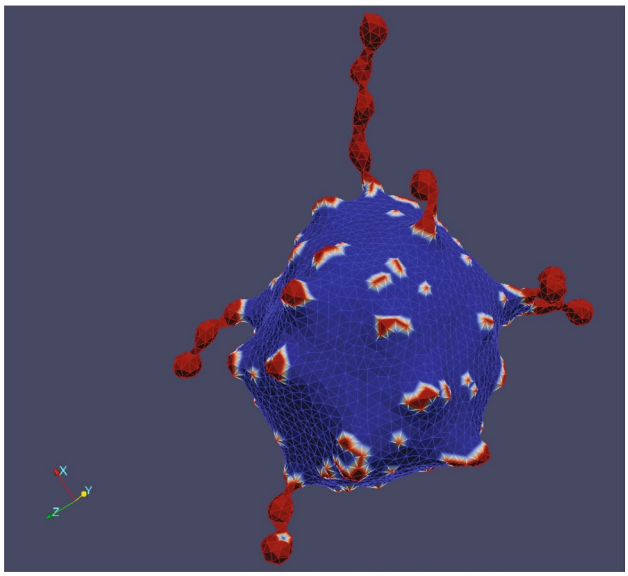

Fig. 8 Non-axisymmetric vesicle shape calculated by MC simulations for the membrane composed of two isotropic constituents. One component has very high intrinsic curvature (marked in *red color*), while the other component has zero intrinsic curvature (marked in *blue color*). The membrane component with high intrinsic curvature is accumulated in the membrane protrusions

in-plane ordering may also better explain the phase transition between the fluid lamellar phase L_α and the inverse hexagonal phase H_{II}. In addition, the deviatoric bending of anisotropic lipid molecules may explain the stability of the inverse hexagonal phase H_{II} at higher temperatures (Perutková et al. 2009). A similar idea was also expressed earlier in Templer (1998), but was not applied to any model calculations.

In membranes possessing orientational ordering, topological defects (TDs) may be formed. TDs are a source of relatively large local elastic penalties. Consequently, they could affect the local membrane shape or even trigger significant biological processes, such as cell fission Jesenek et al. (2013). It has been established that curvature-inducing membrane-nematogens can aggregate spontaneously and change the local shape of the membrane even at low concentrations (Ramakrishnan et al. 2013). The coupling between in-plane nematic order and local curvature on a deformable membrane surface can lead to generation of point defects and line singularities, in turn leading to the production of membrane tubes and branches (Ramakrishnan et al. 2010, 2012).

Conclusions

We performed a numerical study on the impact of different intrinsic curvatures of membrane constituents on the shapes

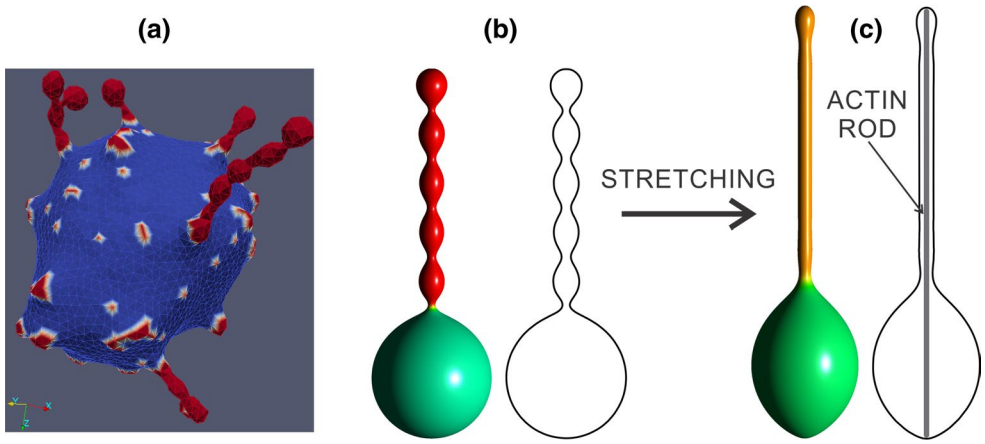

Fig. 9 Vesicle shapes calculated for two-component membrane, where one component has high positive intrinsic curvature. The *red color* represents the highest possible concentration of the membrane component with high intrinsic curvature. The results of the Monte Carlo simulation for non-axisymmetric vesicle shape without actin cytoskeleton is presented in (**a**), while (**b**) and (**c**) show the axisymmetric shapes obtained by the minimization of the free energy functional. The vesicle in (**c**) is stretched by the force of actin filaments

of closed vesicles. We focused mainly on the role of the external force of the cytoskeleton in the formation of membrane tubular protrusions. In cellular systems, such forces may be a consequence of elongating actin filaments. In our theoretical analysis we took into account also the effect of the anisotropic membrane constituents on the formation of membrane tubular protrusions. It was shown that in some cases, external force can induce strong lateral segregation of membrane constituents of different intrinsic curvatures and the concomitant formation of membrane tubular protrusions. The force of actin filaments may stabilize membrane tubular protrusions whose growth is driven by the combined effect of local accumulation of anisotropic membrane constituents and the force originating from the actin cytoskeleton.

The change of the cell/vesicle reduced volume influences the lateral distribution of anisotropic membrane components and the width and length of tubular protrusions. We ascertained that for high and low values of the reduced volume, the isotropic and anisotropic membrane constituents are almost homogeneously distributed/mixed across the whole vesicle surface in the absence of external force (see Figs. 4, 6). This is true for both cases, i.e., with and without considering the entropy of mixing in minimization of the membrane free energy. In the absence of external force the lateral segregation of the isotropic and anisotropic membrane components is stronger if the entropy of mixing is not considered, which results in the formation of thinner and more featured tubular protrusions (Fig. 4). The entropy of mixing enforces membrane constituents of different intrinsic curvatures to intermix, which leads to the formation of wider tubular protrusions, because more isotropic components are distributed also in the vesicle protrusion (Fig. 6).

The lateral segregation of the membrane constituents of different intrinsic curvatures and the consequent formation of membrane tubular protrusions may be facilitated by mechanical force from the actin cytoskeleton. Such force can stretch the vesicle membrane, which results in the formation of a thinner and longer tubular vesicle protrusion and higher degree of lateral segregation of membrane constituents (Fig. 5). The cytoskeleton force can induce the lateral segregation of membrane components and the growth of membrane tubular protrusions on the vesicle surface in the regions which did not have the membrane protrusions before (see the second row in Fig. 7). We predicted a high degree of the lateral segregation of membrane constituents with different intrinsic curvatures if the actin force was applied, even in the case when the mixing entropy was taken into account in the minimization procedure. Note that for high relative vesicle volumes, the intrinsic curvature of membrane components alone is not strong enough to induce the growth of prominent tubular membrane protrusions when the entropy of mixing of different membrane components is taken into account (Fig. 7). In such a case, we have to take into account the external force of actin filaments in order to explain the pronounced segregation of different membrane components and the formation of prominent tubular protrusions (Fig. 7).

To conclude, cytoskeletal mechanical forces can induce the growth of thin tubular membrane protrusions and significantly reduce the effect of the entropy of mixing, reflected in accumulation of anisotropic membrane constituents in tubular membrane protrusions. It should be emphasized that isotropic membrane constituents can induce/stabilize only undulated (necklace-like) membrane protrusions but not tubular membrane protrusions as well (Fig. 9a, b). If undulated membrane protrusions

are stretched by the mechanical force of a cytoskeleton, they are transformed into tubular protrusions (Fig. 9c). Only anisotropic membrane constituents can themselves induce the growth of tubular membrane protrusions in the absence of cytoskeletal force.

References

Ahmed S, Goh WI, Bu W (2010) I-bar domains, irsp53 and filopodium formation. Sem Cell Dev Biol 21:350–356 (Elsevier)

Ayton GS, Voth GA (2010) Multiscale simulation of protein mediated membrane remodeling. Semin Cell Dev Biol 21:357–362 (Elsevier)

Ayton GS, Lyman E, Krishna V, Swenson RD, Mim C, Unger VM, Voth GA (2009) New insights into bar domain-induced membrane remodeling. Biophys J 97(6):1616–1625

Baumgart T, Capraro BR, Zhu C, Das SL (2011) Thermodynamics and mechanics of membrane curvature generation and sensing by proteins and lipids. Annu Rev Phys Chem 62:483

Bernchou U, Brewer J, Midtiby HS, Ipsen JH, Bagatolli LA, Simonsen AC (2009) Texture of lipid bilayer domains. J Am Chem Soc 131(40):14130–14131

Bobrovska N, Góźdź W, Kralj-Iglič V, Iglič A (2013) On the role of anisotropy of membrane components in formation and stabilization of tubular structures in multicomponent membranes. PloS One 8(9):e73941

Bohinc K, Kralj-Iglič V, May S (2003) Interaction between two cylindrical inclusions in a symmetric lipid bilayer. J Chem Phys 119(14):7435–7444

Borghi N, Rossier O, Brochard-Wyart F (2003) Hydrodynamic extrusion of tubes from giant vesicles. Europhys Lett 64(6):837

Boulbitch A (1998) Deflection of a cell membrane under application of a local force. Phys Rev E 57(2):2123

Bo L, Waugh RE (1989) Determination of bilayer membrane bending stiffness by tether formation from giant, thin-walled vesicles. Biophys J 55(3):509–517

Canham PB (1970) The minimum energy of bending as a possible explanation of the biconcave shape of the human red blood cell. J Theor Biol 26(1):61–81

Canham PB (1970) The minimum energy of bending as a possible explanation of the biconcave shape of the human red blood cell. J Theor Biol 26:61–76

Cuvelier D, Derényi I, Bassereau P, Nassoy P (2005) Coalescence of membrane tethers: experiments, theory, and applications. Biophys J 88(4):2714–2726

Davtyan A, Simunovic M, Voth GA (2016) Multiscale simulations of protein-facilitated membrane remodeling. J Struct Biol 196(1):57–63

Downing KH, Nogales E (1998) Tubulin and microtubule structure. Curr Opin Cell Biol 10(1):16–22

Elbaum M, Fygenson DK, Libchaber A (1996) Buckling microtubules in vesicles. Phys Rev Lett 76(21):4078

Emsellem V, Cardoso O, Tabeling P (1998) Vesicle deformation by microtubules: a phase diagram. Phys Rev E 58(4):4807

Fischer TM (1992) Bending stiffness of lipid bilayers. II. Spontaneous curvature of the monolayers. J Phys II 2(3):327–336

Fischer TM (1993) Bending stiffness of lipid bilayers. III. Gaussian curvature. J Phys II 2(3):337–343

Fošnarič M, Iglič A, May S (2006) Influence of rigid inclusions on the bending elasticity of a lipid membrane. Phys Rev E 74(5):051503

Fošnarič M, Iglič A, Slivnik T, Kralj-Iglič V (2008) Flexible membrane inclusions and membrane inclusions induced by rigid globular proteins. Adv Planar Lipid Bilayers Lipos 7:143–168

Fournier J (1996) Nontopological saddle-splay and curvature instabilities from anisotropic membrane inclusions. Phys Rev Lett 76(23):4436

Fournier JB, Galatola P (1998) Bilayer membranes with 2d-nematic order of the surfactant polar heads. Braz J Phys 28(4):329

Frost A, Unger VM, De Camilli P (2009) The bar domain superfamily: membrane-molding macromolecules. Cell 137(2):191–196

Fygenson DK, Marko JF, Libchaber A (1997) Mechanics of microtubule-based membrane extension. Phys Rev Lett 79(22):4497

Gómez-Llobregat J, Elías-Wolff F, Lindén M (2016) Anisotropic membrane curvature sensing by amphipathic peptides. Biophys J 110(1):197–204

Gompper G, Kroll DM (2004) Triangulated-surface models of fluctuating membranes. In: Nelson D, Piran T, Weinberg S (eds) Statistical mechanics of membranes and surfaces. 2nd edn World Scientific, Singapore, pp 359–426

Gompper G, Kroll DM (1996) Random surface discretizations and the renormalization of the bending rigidity. J Phys I 6(10):1305–1320

Gov NS, Gopinathan A (2006) Dynamics of membranes driven by actin polymerization. Biophys J 90(2):454–469

Góźdź WT (2004) Spontaneous curvature induced shape transformation of tubular polymersomes. Langmuir 20:7385–7391

Góźdź WT (2005) Influence of spontaneous curvature and microtubules on the conformations of lipid vesicles. J Phys Chem B 109:21145–21149

Góźdź WT (2006) The interface width of separated two-component lipid membranes. J Phys Chem B 110:21981–21986

Góźdź WT, Bobrovska N, Ciach A (2012) Separation of components in lipid membranes induced by shape transformation. J Chem Phys 137(1):015101

Häckl W, Bärmann M, Sackmann E (1998) Shape changes of self-assembled actin bilayer composite membranes. Phys Rev Lett 80:1786–1789

Hägerstrand H, Mrowczynska L, Salzer U, Prohaska R, Michelsen KA, Kralj-Iglič V, Iglič A (2006) Curvature-dependent lateral distribution of raft markers in the human erythrocyte membrane. Mol Membr Biol 23(3):277–288

Heinrich V, Božič B, Svetina S, Žekš B (1999) Vesicle deformation by an axial load: from elongated shapes to tethered vesicles. Biophys J 76(4):2056–2071

Heinrich V, Waugh RE (1996) A piconewton force transducer and its application to measurement of the bending stiffness of phospholipid membranes. Ann Biomed Eng 24(5):595–605

Helfrich W (1973) Elastic properties of lipid bilayers: theory and possible experiments. Z Naturforsch 28:693–703

Helfrich W, Prost J (1988) Intrinsic bending force in anisotropic membranes made of chiral molecules. Phys Rev A 38(6):3065

Hill TL (1986) An introduction to statistical thermodynamics. Dover Press

Iglič A, Kralj-Iglič V, Majhenc J (1999) Cylindrical shapes of closed lipid bilayer structures correspond to an extreme area difference between the two monolayers of the bilayer. J Biomech 32(12):1343–1347

Iglič A, Veranič P, Batista U, Kralj-Iglič V (2001) Theoretical analysis of shape transformation of v-79 cells after treatment with cytochalasin b. J Biomech 34(6):765–772

Iglič A, Babnik B, Gimsa U, Kralj-Iglič V (2005) On the role of membrane anisotropy in the beading transition of undulated tubular membrane structures. J Phys A-Math Gen 38(40):8527

Iglič A, Hägerstrand H, Veranič P, Plemenitaš A, Kralj-Iglič V (2006) Curvature-induced accumulation of anisotropic

membrane components and raft formation in cylindrical membrane protrusions. J Theor Biol 240(3):368–373

Iglič A, Babnik B, Bohinc K, Fošnarič M, Hägerstrand H, Kralj-Iglič V (2007) On the role of anisotropy of membrane constituents in formation of a membrane neck during budding of a multicomponent membrane. J Biomech 40(3):579–585

Iglič A, Lokar M, Babnik B, Slivnik T, Veranič P, Hägerstrand H, Kralj-Iglič V (2007) Possible role of flexible red blood cell membrane nanodomains in the. Blood Cell Mol Dis 39(1):14–23

Iglič A, Kralj-Iglič V, Drobne D (2015) Nanostructures in Biological Systems: theory and applications. Pan Stanford Publishing Pte. Ltd

Isambert H, Venier P, Maggs AC, Fattoum A, Kassab R, Pantaloni D, Carlier MF (1995) Flexibility of actin filaments derived from thermal fluctuations. effect of bound nucleotide, phalloidin, and muscle regulatory proteins. J Biol Chem 270(19):11437–11444

Israelachvili JN (2011) Intermolecular and surface forces: revised third edition. Academic Press

Jelerčič U, Gov NS (2015) Pearling instability of membrane tubes driven by curved proteins and actin polymerization. Phys Biol 12(6):066022

Jesenek D, Perutková S, Góźdź W, Kralj-Iglič V, Iglič A, Kralj S (2013) Vesiculation of biological membrane driven by curvature induced frustrations in membrane orientational ordering. Int J Nanomed 8:677–687

Kabaso D, Bobrovska N, Góźdź W, Gov N, Kralj-Iglič V, Veranič P, Iglič A (2012) On the role of membrane anisotropy and bar proteins in the stability of tubular membrane structures. J Biomech 45(2):231–238

Kabaso D, Bobrovska N, Góźdź W, Gongadze E, Kralj-Iglič V, Zorec R, Iglič A (2012) The transport along membrane nanotubes driven by the spontaneous curvature of membrane components. Bioelectrochemistry 87:204–210

Kralj-Iglič V, Svetina S, Žekš B (1996) Shapes of bilayer vesicles with membrane embedded molecules. Eur Biophys J 24(5):311–321

Kralj-Iglič V, Heinrich V, Svetina S, Žekš B (1999) Free energy of closed membrane with anisotropic inclusions. Eur Phys J B 10:5–8

Kralj-Iglič V, Iglič A, Hägerstrand H, Peterlin P (2000) Stable tubular microexovesicles of the erythrocyte membrane induced by dimeric amphiphiles. Phys Rev E 61:4230–4234

Kralj-Iglič V, Iglič A, Gomišček G, Sevšek F, Arrigler V, Hägerstrand H (2002) Microtubes and nanotubes of a phospholipid bilayer membrane. J Phys A-Math Gen 35(7):1533–1549

Kralj-Iglič V, Remškar M, Vidmar G, Fošnarič M, Iglič A (2002) Deviatoric elasticity as a possible physical mechanism explaining collapse of inorganic micro and nanotubes. Phys Lett A 296(2):151–155

Kralj-Iglič V, Hägerstrand H, Veranič P, Jezernik K, Babnik B, Gauger DR, Iglič A (2005) Amphiphile-induced tubular budding. Eur Biophys J 34(8):1066–1070

Kralj-Iglič V, Babnik B, Gauger D, May S, Iglič A (2006) Quadrupolar ordering of phospholipid molecules in narrow necks of phospholipid vesicles. J Stat Phys 125(3):727–752

Kralj-Iglic V (2012) Stability of membranous nanostructures: a possible key mechanism in cancer progression. Int J Nanomed 7:3579–3596

Kulkarni CV (2012) Lipid crystallization: from self-assembly to hierarchical and biological ordering. Nanoscale 4(19):5779–5791

Liu AP, Richmond DL, Maibaum L, Pronk S, Geissler PL, Fletcher DA (2008) Membrane-induced bundling of actin filaments. Nat Phys 4(10):789–793

Lubensky T, Prost J (1992) Orientational order and vesicle shape. J Phys II 2(3):371–382

MacKintosh FC, Lubensky TC (1991) Orientational order, topology, and vesicle shapes. Phys Rev Lett 67:1169–1172

McMahon HT, Gallop JL (2005) Membrane curvature and mechanisms of dynamic cell membrane remodelling. Nature 438(7068):590

Mesarec L, Góźdź W, Kralj Iglič V, Kralj S, Iglič A (2016) Closed membrane shapes with attached bar domains subject to external force of actin filaments. Colloid Surface B 141:132–140

Miyata H, Nishiyama S, Akashi KI, Kinosita K (1999) Protrusive growth from giant liposomes driven by actin polymerization. P Natl Acad Sci USA 96(5):2048–2053

Noguchi H (2016) Membrane tubule formation by banana-shaped proteins with or without transient network structure. Scientific Reports 6

Penič S, Iglič A, Bivas I, Fošnarič M (2015) Bending elasticity of vesicle membranes studied by Monte Carlo simulations of vesicle thermal shape fluctuations. Soft Matter 11(25):5004–5009

Perutková Š, Daniel M, Dolinar G, Rappolt M, Kralj-Iglič V, Iglič A (2009) Stability of the inverted hexagonal phase. Adv Planar Lipid Bilayers Liposomes 9:237–278

Perutková Š, Kralj-Iglič V, Frank M, Iglič A (2010) Mechanical stability of membrane nanotubular protrusions influenced by attachment of flexible rod-like proteins. J Biomech 43(8):1612–1617

Perutková Š, Daniel M, Rappolt M, Pabst G, Dolinar G, Kralj-Iglič V, Iglič A (2011) Elastic deformations in hexagonal phases studied by small-angle X-ray diffraction and simulations. Phys Chem Chem Phys 13(8):3100–3107

Peter BJ, Kent HM, Mills IG, Vallis Y, Butler PJG, Evans PR, McMahon HT (2004) Bar domains as sensors of membrane curvature: the amphiphysin bar structure. Science 303(5657):495

Ramakrishnan N, Kumar PS, Ipsen JH (2010) Monte Carlo simulations of fluid vesicles with in-plane orientational ordering. Phys Rev E 81(4):041922

Ramakrishnan N, Kumar PBS, Ipsen JH (2011) Modeling anisotropic elasticity of fluid membranes. Macromol Theor Simul 20(7):446–450

Ramakrishnan N, Ipsen JH, Kumar PS (2012) Role of disclinations in determining the morphology of deformable fluid interfaces. Soft Matter 8(11):3058–3061

Ramakrishnan N, Kumar PS, Ipsen JH (2013) Membrane-mediated aggregation of curvature-inducing nematogens and membrane tubulation. Biophys J 104(5):1018–1028

Rappolt M, Hodzic A, Sartori B, Ollivon M, Laggner P (2008) Conformational and hydrational properties during the-to-and-to hii-phase transition in phosphatidylethanolamine. Chem Phys Lipids 154(1):46–55

Saarikangas J, Zhao H, Pykäläinen A, Laurinmäki P, Mattila PK, Kinnunen PK, Butcher SJ, Lappalainen P (2009) Molecular mechanisms of membrane deformation by i-bar domain proteins. Curr Biol 19(2):95

Scita G, Confalonieri S, Lappalainen P, Suetsugu S (2008) Irsp53: crossing the road of membrane and actin dynamics in the formation of membrane protrusions. Trends Cell Biol 18(2):52–60

Seifert U (1997) Configurations of fluid membranes and vesicles. Adv Phys 46(1):13–137

Shlomovitz R, Gov NS (2008) Physical model of contractile ring initiation in dividing cells. Biophys J 94(4):1155–1168

Simons K, Sampaio JL (2011) Membrane organization and lipid rafts. Cold Spring Harbor Perspect Biol 3(10):a004,697

Simunovic M, Voth GA, Callan-Jones A, Bassereau P (2015) When physics takes over: Bar proteins and membrane curvature. Trends Cell Biol 25(12):780–792

Singer SJ, Nicolson GL (1972) The fluid mosaic model of the structure of cell membranes. Science 175(4023):720

Smith G, Sirota E, Safinya C, Clark NA (1988) Structure of the l β phases in a hydrated phosphatidylcholine multimembrane. Phys Rev Lett 60(9):813

Suetsugu S (2010) The proposed functions of membrane curvatures mediated by the bar domain superfamily proteins. J Biochem 148(1):1–12

Templer RH (1998) Thermodynamic and theoretical aspects of cubic mesophases in nature and biological amphiphiles. Curr Opin Colloid Interface Sci 3(3):255–263

Umeda T, Nakajima H, Hotani H (1998) Theoretical analysis of shape transformations of liposomes caused by microtubule assembly. J Phys Soc Jpn 67(2):682–688

Veksler A, Gov NS (2007) Phase transitions of the coupled membrane-cytoskeleton modify cellular shape. Biophys J 93(11):3798–3810

Venier P, Maggs AC, Carlier MF, Pantaloni D (1994) Analysis of microtubule rigidity using hydrodynamic flow and thermal fluctuations. J Biol Chem 269(18):13353–13360

Wade RH, Hyman AA (1997) Microtubule structure and dynamics. Curr Opin Cell Biol 9(1):12–17

Walani N, Torres J, Agrawal A (2014) Anisotropic spontaneous curvatures in lipid membranes. Phys Rev E 89(6):062715

Yang C, Hoelzle M, Disanza A, Scita G, Svitkina T (2009) Coordination of membrane and actin cytoskeleton dynamics during filopodia protrusion. PloS One 4(5):e5678

Zimmerberg J, Kozlov MM (2006) How proteins produce cellular membrane curvature. Nat Rev Mol Cell Biol 7(1):9–19

Zimmerberg J, McLaughlin S (2004) Membrane curvature: how bar domains bend bilayers. Curr Biol 14(6):R250–R252